analytical chemistry

Article

pubs.acs.org/ac

Targeted Quantification of C-Reactive Protein and Cystatin C and Its Variants by Immuno-MALDI-MS

Klaus Meyer*[,†] and Per Magne Ueland[‡,§]

[†]Bevital AS, Laboratory Building, 9th Floor, Jonas Lies veg 87, 5021 Bergen, Norway

[‡]Department of Clinical Science, University of Bergen, 5021 Bergen, Norway

[§]Laboratory of Clinical Biochemistry, Haukeland University Hospital, 5021 Bergen, Norway

Supporting Information

ABSTRACT: The most common technologies for quantitative determination of protein biomarkers are immunoassays, which exist in various formats. Immunoassays offer sensitive and fast protein quantification, but can hardly discriminate between protein variants. Post-translational modifications and genetic variants increase protein microheterogeneity and may play important roles in biological processes. Mass spectrometry combined with immunoaffinity enrichment detects protein microheterogeneity and can quantify different isoforms. We here present an immuno-MALDI-MS approach for the combined quantification of two important biomarkers of inflammation and renal function, C-reactive protein (CRP) and cystatin C, respectively. Antibodies were immobilized onto reversed-phase tips, which allows easy and flexible sample processing. Quantification was performed in singleplex and duplex assays, and characteristics were evaluated for different internal standards, i.e., PEGylated and polyhistidine-tagged proteins. The best performances were obtained for polyhistidine-tagged standards with respect to limits of detection (CRP, 0.10 μg/mL; cystatin C, 0.003 μg/mL) and coefficients of variation (CRP, 2.4−7.0%; cystatin C, 3.0−8.9%). The methods were benchmarked against immunoturbidimetry and nephelometry and demonstrated good between-assay agreement (R^2 = 0.989 for CRP; R^2 = 0.939 for cystatin C). Several variants of cystatin C were identified and quantified, while none were observed for CRP. This immuno-MALDI method describes a novel approach for targeted quantitative investigation of protein microheterogeneity and is well suited for assessment of biomarker status in precious samples from biobanks due to its low sample consumption.

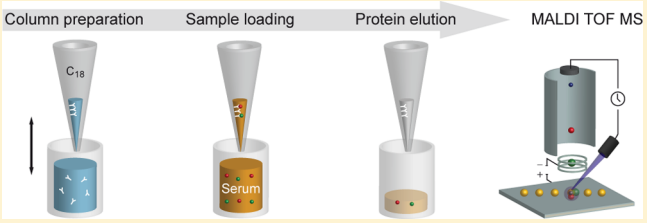

Protein biomarkers for the diagnosis and risk assessment of diseases have attracted increasing interest during the past several years. The growing activity in proteomics has generated a large number of candidate biomarkers, and the expectations to discover novel biomarkers are high.[1−5] Potential markers have to be verified and validated in clinical studies with respect to the disease of interest. Protein microheterogeneity, mainly caused by post-translational modifications, dramatically increases the diversity of the proteome and therefore has become an important topic in clinical proteomics.[6−9] Protein isoforms differ slightly, but can play important roles in biological processes and vary between different pathologies and individuals. Therefore, knowledge about protein microheterogeneity is crucial in personalized medicine and for comparing study results obtained by different technologies.

Investigation of protein microheterogeneity by traditional immunoassays such as Western blotting and enzyme-linked immunosorbent assay (ELISA) is difficult.[10,11] Either these methods capture the wild type together with the variants, but cannot discriminate between them, or the antibody does not recognize the modified proteins. Although modern array-based immunoassays enable multiplexing of numerous proteins,[12,13] the production of highly specific antibodies against protein isoforms with minor structural differences, remains a challenge.

Mass spectrometry (MS) has become a powerful technology for the characterization and quantification of proteins and their structural modifications.[14−16] Electrospray ionization (ESI) and matrix-assisted laser desorption/ionization (MALDI) coupled to triple-quadrupole, orbitrap, or time-of-flight (TOF) analyzers have become the most commonly used techniques in proteomics. While in the early years of proteomics these techniques were applied in protein biomarker discovery, the field now includes targeted proteomics for investigation of known proteins and validation of biomarkers in large sample cohorts.[17−22] Most approaches are based on bottom-up methods and use proteolytic digestion for structural identification, which hampers discrimination of post-translational modifications.

In contrast, the combination of immunoaffinity enrichment and detection of the intact protein by MALDI delivers unambiguous protein characterization at high sample throughput. Different immuno-MALDI formats have been established using gold-coated chips with self-assembled monolayers,[23] functionalized superparamagnetic nanoparticles,[24,25] or affinity pipet tips.[26,27] Especially, the so-called mass spectrometric

Received: February 6, 2014
Accepted: May 15, 2014
Published: May 21, 2014

   dx.doi.org/10.1021/ac500704y | Anal. Chem. 2014, 86, 5807−5814

immunoassay (MSIA) has been applied to numerous proteins and has recently become commercially available, utilizing universal binding ligands.[11,28−35]

Quantification by MALDI-MS is challenging because of its poor reproducibility, and the use of internal standards (ISs) is mandatory to obtain high assay precision. For intact protein quantification uniformly-isotope-labeled proteins represent the "gold standard" as the IS, since they are structurally identical to the target protein, but differ in molecular mass.[28,29] However, the production of uniformly-isotope-labeled proteins is difficult and costly. Alternatively, endogenous and exogenous proteins can serve as the IS for relative and absolute quantification, respectively.[19,25,32,38] The assays are carried out with at least two different antibodies, one specific for the target protein and one for the IS. Only one competitive immunoassay has been described so far using a recombinant variant of the target protein as the IS.[30]

C-reactive protein (CRP) and cystatin C (CysC) are important biomarkers in both clinical and epidemiological studies. CRP belongs to the protein family of pentraxins, which is characterized by calcium-dependent ligand binding of five monomers (23 kDa) forming a radial symmetric ring.[31,32] CRP is the major marker for systemic inflammation and is produced in hepatocytes, mainly under the transcriptional control of cytokine IL-6. Low levels of the so-called high-sensitivity (hs) CRP (<10 μg/mL), typically found in generally healthy subjects, have been related to higher risks of cardiovascular events,[33−36] stroke,[36,37] cancer,[38−40] and metabolic syndrome.[41,42] Cystatin C is a nonglycosylated cysteine protease inhibitor with a molecular mass of 13 kDa.[43] Since it is produced at a constant rate by nucleated cells and freely filtered by the renal glomerulus, serum cystatin C is an indicator for renal dysfunction.[44,45] There is growing evidence that cystatin C is a more specific indicator of the glomerular filtration rate than creatinine, because the levels are less dependent on age, sex, and muscle mass. In addition, cystatin C has been acknowledged as a marker of elevated risk of death from myocardial infarction,[46,47] stroke,[48] and metabolic syndrome.[49] Higher levels of cystatin C and the presence of certain isoforms have been related to neurological and cerebral disorders such as cerebral amyloid angiopathy,[50] amyotrophic lateral sclerosis,[51] multiple sclerosis,[52] and Alzheimer's disease.[53] More than a dozen cystatin isoforms have been detected so far, in both serum[19] and cerebrospinal fluid.[54]

We here present a novel immuno-MALDI-TOF-MS approach for the quantification of CRP and cystatin C and its variants. Antibodies are immobilized to C_{18} reversed-phase pipet tips, which enables flexible assay designs and easy work flow. Quantification is performed using two different types of labeled recombinant protein standards, and the assay is carried out in singleplex and duplex formats. The low sample volume consumption of 20 μL makes it suitable for studies based on precious samples stored in biobanks.

EXPERIMENTAL SECTION

Materials. Recombinant human CRP was provided by R&D Systems (Abingdon, U.K.). Methyl-$(PEG)_4$ *N*-hydroxysuccinimide ester, used for PEGylation of CRP, was purchased from Thermo Scientific (Rockford, IL). Polyhistidine-tagged recombinant human CRP (CRP-HIS) and cystatin C (CysC-HIS) were purchased from Acro-Biosystems (Newark, DE) (CRP-H5226) and BioVendor (Bmo, Czech Republic) (RD172009100-H), respectively. The additional amino acid sequences were His_6 for CRP-HIS and MetLysHis$_6$Ala for CysC-HIS. Horse serum was from Abcam (Cambridge, U.K.), ZipTips (C_{18}) were from Millipore (Billerica, MA), polyclonal anti-CRP (12.4 μg/mL) was from Merck (Darmstadt, Germany), polyclonal anticystatin C (2.6 μg/mL) was from Hytest (Turku, Finland), phosphate buffered saline (PBS) was from G-Bioscience (St. Louis, MO), and G-25 PD MidiTrap columns were from GE Healthcare (Oslo, Norway). Ultrapure water was obtained from a Milli-Q system (Billerica, MA). Acetonitrile, trifluoroacetic acid (TFA), bovine serum albumin (BSA), and 2,5-dihydroxyacetophenone (2,5-DHAP) were purchased from Sigma (Oslo, Norway).

Reference Samples. The Laboratorium for Klinisk Biokjemi (LKB) of the Haukeland University Hospital (Bergen, Norway) and the Institut fur Klinische Chemie of the Otto von Guericke University Magdeburg (Magdeburg, Germany) provided clinical serum samples for method comparison. While samples from LKB covered the hs-CRP range from 0.1 to 10 μg/mL (N = 87), samples from Magdeburg were collected randomly from routine analyses of CRP and cystatin C (N = 96). CRP was analyzed in both laboratories using a Tina-quant immunoturbidimetry assay from Roche/Hitachi (Basel, Switzerland), while cystatin C was quantified by a nephelometry assay from Siemens (Munchen, Germany). All samples were stored at −80 °C. This part of the study is in the quality control (QC) category, which under the current Norwegian regulations is exempt from review by the institutional review board.

Calibrants. Human reference sera DA474/IFCC and DA471 were purchased from the Reference Materials Unit of the European Commission Joint Research Centre (Geel, Belgium) and were used as calibrants for CRP and cystatin C, respectively. While the DA474/IFCC material was collected from pooled human serum samples, DA471 was produced by spiking human sera with recombinant cystatin C. Two sets of calibrants each consisting of eight samples were prepared from the reference material. For the CRP singleplex method DA474/IFCC (41.2 μg/mL) was diluted with horse serum to final concentrations of 10.30, 5.15, 2.57, 1.29, 0.64, 0.32, 0.16, and 0 μg/mL. The calibrants for the duplex assay were prepared by diluting DA474/IFCC and DA471 (11.16 μg/mL) to a CRP/cystatin C concentration series of 10.30/5.58, 5.15/2.79, 2.57/1.39, 1.29/0.69, 0.64/0.35, 0.32/0.17, 0.16/0.09, and 0 μg/mL. Aliquots of the prepared calibrants were stored at −80 °C. Calibrants were thawed and vortexed before use.

Internal Standards. A 200 μg sample of lyophilized human recombinant CRP was dissolved in 500 μL of PBS and mixed with 12 μL of methyl-$(PEG)_4$ ester to produce PEGylated CRP. After 30 min the reaction was terminated and the CRP-PEG was desalted using G-25 spin columns, which also removed excess *N*-hydroxysuccinimide ester and its leaving group. The CRP-PEG was further diluted in PBS to a final concentration of 16 μg/mL. For the duplex assay the polyhistidine-tagged variants of CRP and cystatin C were mixed together in PBS to a final concentration of 2.5 and 1 μg/mL, respectively. Concentrations of all internal standards were adjusted to achieve equivalent signal intensities from the IS and target protein at median levels of a healthy population (CRP, 2.1 μg/mL; cystatin C, 0.8 μg/mL).[55,56] Internal standards were stored at 4 °C and were vortexed before use.

Sample Purification. Column preparation and protein enrichment were carried out on a Cybi-Disk robot from CyBio AG (Jena, Germany). All reagents were filled into 96-well microtiter plates using a Beckman Coulter (Brea, CA) Biomek 2000 robot and placed into the CybiDisk. Immunoaffinity enrichment was performed according to a modified protocol of

dx.doi.org/10.1021/ac500704y | Anal. Chem. 2014, 86, 5807−5814

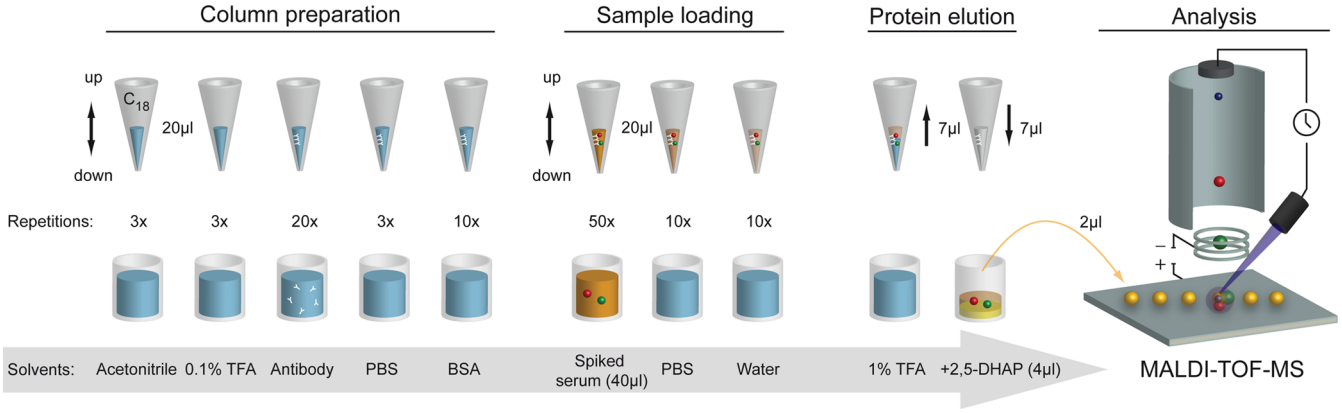

Figure 1. Work flow of the immuno-MALDI method. Miniaturized C_{18} columns (ZipTips) served as the solid phase for antibody immobilization, and reagents were rinsed through the tips by repeated pipetting. Column preparation started with equilibration with 100% acetonitile and 0.1% TFA, followed by immobilization with concentrated antibody, washing with PBS, and blocking residual C_{18} groups by BSA. ZipTips were incubated with serum samples and washed with PBS and water. The purified proteins were eluted from the column by 1% TFA, mixed with the 2,5-DHAP matrix, and analyzed by MALDI-MS.

Applied Biosystems.[57] The method started with equilibration of the ZipTips by aspirating and dispensing 20 μL of acetonitrile (100%) three times, followed by three repetitions with 20 μL of TFA (0.1%) (Figure 1). Concentrated antibody was bound to the C_{18} material by aspiration and dispensing 10 μL of the antibody solution 20 times. Notably, antibodies of different manufacturers have to be tested, since some antibodies can denature when bound to reversed-phase material. For the duplex assay concentrated antibodies against CRP and cystatin C were mixed in a ratio of 4:5, which delivered protein signal spectra of comparable intensities. Unbound antibody was removed from the columns by rinsing the tip with PBS (20 μL, three repetitions). Residual free C_{18} groups were blocked using a 10 mg/mL solution of BSA (20 μL, 10 repetitions), and the columns were then ready for sample loading. Human sera (20 μL) were spiked with the internal standard (20 μL), vortexed, and centrifuged for 5 min at 6000*g*. Spiked calibrants or samples were loaded onto the ZipTips (20 μL) by aspiration and dispensing 50 μL through the column, followed by column washing with PBS (20 μL, 10 repetitions) and H_2O (20 μL, 10 repetitions). As the final step, the bound proteins were eluted from the ZipTip with 7 μL of 1% TFA and prepared for MALDI-MS.

MALDI-MS. 2,5-DHAP was prepared as the MALDI matrix as described by Wenzel et al.[58] We modified this protocol with respect to automated sample spotting using a Cybi-Disk robot and Bruker (Bremen, Germany) BigAnchor chip targets. The concentration of the DHAP matrix was reduced to 7.6 μg/mL. Instead of 100% ethanol, a mixture of ethanol and acetonitrile (1:3) was used to increase the solubility, surface tension, and rate of evaporation, thus producing a more compact and homogeneous matrix/sample crystallization (data not shown). A 4 μL sample of the 2,5-DHAP solution was added to the eluted sample and mixed vigorously by the Cybi-Disk. In addition, the pipets rubbed against the microtiter wells, thereby generating a fine matrix/sample suspension. A 2 μL sample of this suspension was dispensed on a BigAnchor 384 target and dried at room temperature (Figure 1).

MALDI analyses were performed on a Bruker UltraFlextreme instrument in positive ion reflector mode at 25 kV acceleration voltage. Each sample was desorbed by 8000 laser shots at a frequency of 1 kHz, applied at 500 shots per sample spot. The laser intensity was fixed at 40%, and the detector voltage was 3080 V. The laser beam was rastered over the surface using a hexagon pattern. Acquired spectra were smoothed with a Savitzky Golay filter and background subtracted by the Tophat filter using Bruker's flexAnalysis software. Signal intensities were determined from the peak height, which appeared to be more accurate than the peak areas (data not shown).

Assay Characteristics. Two different assays were designed: a singleplex version for quantification of CRP using PEGylated recombinant human CRP as the IS (CRP/CRP-PEG) and a duplex assay for quantification of CRP and cystatin C using polyhistidine-tagged protein standards (CRP/CRP-HIS, CysC/CysC-HIS). Characteristic mass peaks were identified for PBS, blank horse serum, calibrants, and human serum samples spiked with PEGylated or polyhistidine-tagged IS processed through the protocol established for immunoaffinity enrichment. Three different standard curves were prepared for the singleplex and duplex assays by spiking the calibrants with the relevant internal standards (20 μL:20 μL). Replicates of nine samples were analyzed for each concentration, and the peak ratios of the target protein to the IS were plotted against the concentrations.

The limit-of-detection (LOD) was calculated as LOD = LOB + 1.645($SD_{low\text{-}concn\ sample}$), where LOB is the limit-of-blank = $mean_{blank}$ + 1.645(SD_{blank}), as described by Armbuster et al.[59] The limit-of-quantification (LOQ) was estimated as the lowest concentration of the analyte that could be quantified with a coefficient of variation (CV) of 20%.

Assay precisions were calculated by repeated analyses of human serum samples at three different levels of CRP and cystatin C. Twelve replicates were quantified for determination of the within-day CV, while between-day CVs were determined by four replicates measured on 10 different days.

Method comparison was performed by Passing–Bablok regression[60] and Bland–Altman plots.[61] Passing–Bablok regression was performed by plotting the concentrations obtained by immuno-MALDI against those obtained with reference techniques. The slope and intercept did not differ significantly from each other if their 95% confidence intervals (CIs) included 1 and 0, respectively. For the Bland–Altman plots the relative differences between MALDI-MS and the reference methods were plotted against their mean levels.

Finally, different ratios of cystatin C isoforms (CysC/CysC-3ProOH; truncated/nontruncated) were tested for correlation

dx.doi.org/10.1021/ac500704y | *Anal. Chem.* 2014, 86, 5807–5814

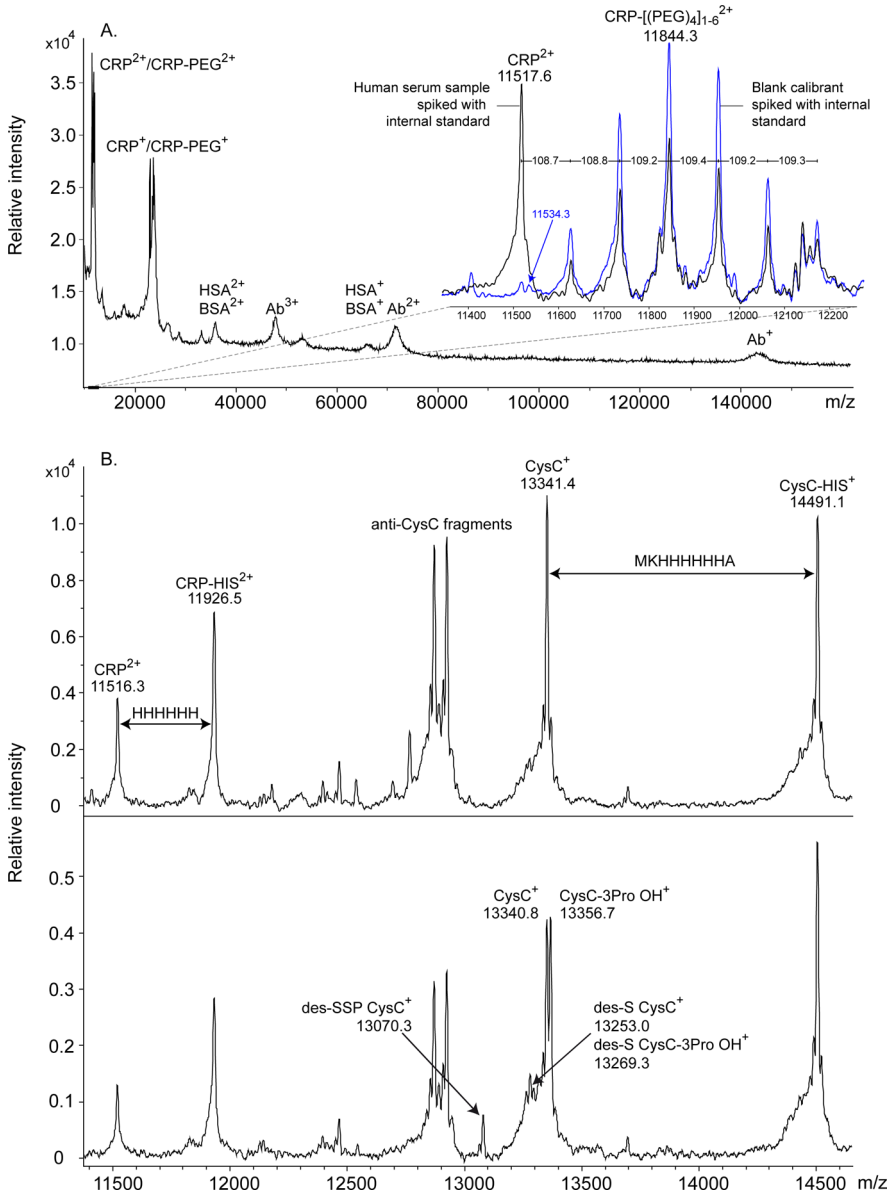

Figure 2. (A) Immuno-MALDI-MS spectrum of CRP in human serum using PEGylated CRP (CRP-PEG) as the IS. The spectrum was acquired in positive reflector ion mode and is plotted from 10 to 150 kDa. Weak signals of anti-CRP antibody and serum albumin are observed in the range above 30 kDa, while the lower mass range shows singly and doubly charged CRP and CRP-PEG. The doubly charged ions represent the dominant peaks and were chosen for quantification. CRP-PEG was detected as a CRP-$[(PEG)_4]_{1-6}$ peak distribution, and its doubly charged peak pattern is magnified in the inset. CRP-PEG containing three PEG groups represents the most abundant peak of the distribution and was chosen for quantification. The additional blue trace shows a spectrum from a blank calibrant sample spiked with CRP-PEG. A weak signal of CRP is observed which originates from the PEGylation reaction. Since its contribution is about 0.1 μg/mL, this interference does not affect CRP quantification. (B) Immuno-MALDI-MS spectra for the CRP/CysC duplex assay including CRP and cystatin C and their polyhistidine-tagged derivatives as the internal standards. The upper panel shows a typical mass spectrum of a calibrant sample including peaks of recombinant CRP and cystatin C and the standards CRP-HIS and CysC-HIS, respectively. Other signals are related to low-mass fragments from anti-CysC antibody. The lower panel shows the spectrum of a human serum sample containing additional signals for cystatin C isoforms, i.e., CysC-3Pro-OH, des-S CysC, des-S CysC-3Pro-OH, and des-SSP CysC.

with total cystatin C levels using Spearman's rank test (using SPSS version 21).

RESULTS AND DISCUSSION

Characterization of Mass Spectra. The linear mode delivered the highest signal-to-noise ratios, but all MALDI-TOF spectra were acquired in reflector ion mode, because high-resolution mass spectra were required to resolve the complex patterns of PEGylated CRP and cystatin C isoforms. An unprocessed positive reflector ion mode spectrum of a human serum sample quantified by the CRP/CRP-PEG assay is shown in Figure 2A, spanning the mass range from 10 to 150 kDa. CRP was detected as its monomeric isoform of about 23 kDa mass together with the PEGylated internal standard. No other variants of CRP were identified during assay development, which is in agreement with earlier investigations.[10] The pentameric form of CRP (115 kDa) was not observed in the higher mass range and may be dissociated during sample preparation.

The most dominant peak of CRP was obtained from the doubly charged ion and thus was chosen for quantification. The

dx.doi.org/10.1021/ac500704y | Anal. Chem. 2014, 86, 5807−5814

inset in Figure 2A, upper right corner, shows the magnified mass spectrum of the doubly charged signals of CRP and CRP-PEG. The mass peak at 11517.6 Da represented the CRP^{2+} ion, while the peaks in the range of 11600−12200 Da represented CRP-PEG and consisted of up to six $(PEG)_4$ units, each of 218 Da. CRP labeled with three $(PEG)_4$ units (11844.3 Da) had the highest abundance and was chosen as the internal standard for quantification. The overlaid spectrum (blue line) shows a blank sample (horse serum) spiked with CRP-PEG. A weak signal related to residual CRP from the internal standard could be detected, but the estimated contribution of 0.1 μg/mL by this contamination was negligible. Horse CRP gave a signal at 11534.3 Da (http://www.uniprot.org/uniparc/UPI0001560F76), which, however, did not interfere with CRP quantification.

A positive ion spectrum of a calibrant sample for the CRP/CysC duplex assay is shown in the upper panel of Figure 2B, with labels on the signals of the target proteins and internal standards. For CRP the doubly charged ion species (11516.3 and 11926.5 Da) represented again the major peaks, while signal intensities of cystatin C did not differ for ions carrying one or two positive charges (doubly charged peaks not shown). Signals related to cystatin C were located in the mass range from 12 to 15 kDa and consisted of CysC (13341.4 Da) and CysC-HIS (14491.1 Da). The spectrum in the lower panel was obtained from a human serum sample and contained additional peaks from post-translational cystatin C variants. The major signal of cystatin C presented as a peak doublet (13340.8 and 13356.7 Da) with each component of similar abundances caused by a hydroxylated form (hydroxyproline at position 3) of cystatin C, as described earlier.[62] Other isoforms truncated at their N-terminal were found at 13070.3 Da (des-SSP CysC), 13253.0 Da (des-S CysC), and 13269.3 Da (des-S CysC 3Pro-OH) and confirm earlier findings by Trenchevska et al.[19]

Standard Curves. The standard curve for CRP/CRP-PEG was obtained by plotting the ion signal ratios of CRP^{2+} to $CRP\text{-}PEG^{2+}$ against the CRP concentration ranging from 0 to 10 μg/mL (Supporting Information Figure S-1A). The obtained curve was nonlinear and fitted by a polynomial function of second order (R^2 = 0.996). Preparation of several standard curves showed that a polynomial function of second order was typical for this immuno-MALDI assay. Especially, the settings of the time-of-flight detector strongly determined the coefficients of the quadratic polynomial function (data not shown). Parts B and C of Figure S-1 show the results of the duplex method of CRP and cystatin C using polyhistidine-tagged proteins as the IS. The curve for $CRP^{2+}/CRP\text{-}HIS^{2+}$ (Figure S-1B) demonstrated better linearity, lower variation, and a better fit (R^2 = 0.999) compared to that for CRP-PEG.

The lower performance of CRP-PEG may be explained by three factors. First, it can be assumed that CRP-PEG possesses lower antigenicity than CRP-HIS, because it carries three $(PEG)_4$ units, randomly bound to the primary amides. In contrast, CRP-HIS has higher structural similarity to CRP and probably antigenicity similar to that of CRP. Second, spectral processing, i.e., background subtraction, may be less accurate for the narrow distribution of CRP-PEG species compared to a single peak as obtained with CRP-HIS. Homogeneity of the sample/matrix crystallization is a third factor, which can differ between the assay formats. 2,5-DHAP is an excellent matrix for protein analysis,[58] and we could show that this matrix is also well-suited for quantification in combination with anchor targets, but the lower hydrophobicity of CRP-PEG may impair cocrystallization and therefore cause more heterogeneous MALDI preparation.

The standard curve of cystatin C was plotted from 0 to 6 μg/mL (Supporting Information Figure S-1C), covering the clinically relevant concentration range. The curve showed a point of inflection and thus was fitted separately for two segments to obtain optimal regression. Concentrations <1.4 μg/mL followed a positive polynomial function of second order (R^2 = 0.996) and concentrations >1.4 μg/mL a negative polynomial function of second order (R^2 = 0.931). This segmented curve may reflect saturation of the antigen−antibody capacity.

Assay Performance. The limits of detection and quantification were determined for both assay formats. The CRP/CRP-HIS format delivered lower limits (LOD = 0.10 μg/mL; LOQ = 0.16 μg/mL) than CRP/CRP-PEG (LOD = 0.16 μg/mL; LOQ = 0.32 μg/mL), probably due to the higher antigenicity of CRP-HIS. In addition, CRP-PEG consists of species with 1−6 PEG units, and thus, the total concentration of CRP-PEG was about 6 times higher than for CRP-HIS to achieve similar signal ratios with CRP. As a consequence, the antibody capacity for CRP was lower for the CRP/CRP-PEG assay. The lowest limits of detection and quantification were achieved for the CysC/CysC-HIS format and were 0.003 and 0.009 μg/mL, respectively.

The assay precisions in terms of between- and within-day variations are shown in Table 1. Assays demonstrated high precision with CVs between 11.7% and 2.4%. Both within- and between-day variations were lower for CRP/CRP-HIS than CRP/CRP-PEG. Notably, the lowest CVs were observed for samples in the midrange concentrations. At these serum levels, the mass peaks of the target proteins and ISs had comparable signal intensities and, due to the limited dynamic range in MALDI-TOF-MS, provided the best signal-to-noise ratios.

Table 1. Within- and Between-Day Variations for Singleplex and Duplex Methods[a]

singleplex method		duplex method			
CRP		CRP		tCysC[b]	
concn (μg/mL)	CV (%)	concn (μg/mL)	CV (%)	concn (μg/mL)	CV (%)
Within-Day Variation					
0.6	8.4	0.6	5.4	0.9	4.6
1.5	5.4	1.5	3.3	1.1	3.0
11.4	6.5	11.4	5.5	6.8	8.9
Between-Day Variation					
1.6	11.7	1.3	3.3	0.9	8.0
3.1	7.0	4.3	2.4	1.2	4.7
6.2	8.4	12.0	7.0	6.1	6.7

[a]Internal standards: CRP-PEG in singleplex assay and CRP-HIS/CysC-HIS in duplex assay. [b]Total cystatin C = sum of all cystatin C isoforms.

The throughput of the method was 96 × 4 samples per 8 h working day. A 4-fold higher throughput is possible by upgrading the Cybi-Disk and the MALDI anchor target to the 384 pipet format.

We validated the immuno-MALDI-MS assays for CRP and cystatin C by comparison with established techniques using two sets of human reference sera. The first reference set was used for validation of both assay formats for hs-CRP (Figure 3A,B). Linear regression demonstrated good agreement for CRP/CRP-PEG (R^2 = 0.981) and CRP/CRP-HIS (R^2 = 0.989) with turbidimetry, while Passing−Bablok regression showed signifi-

dx.doi.org/10.1021/ac500704y | Anal. Chem. 2014, 86, 5807−5814

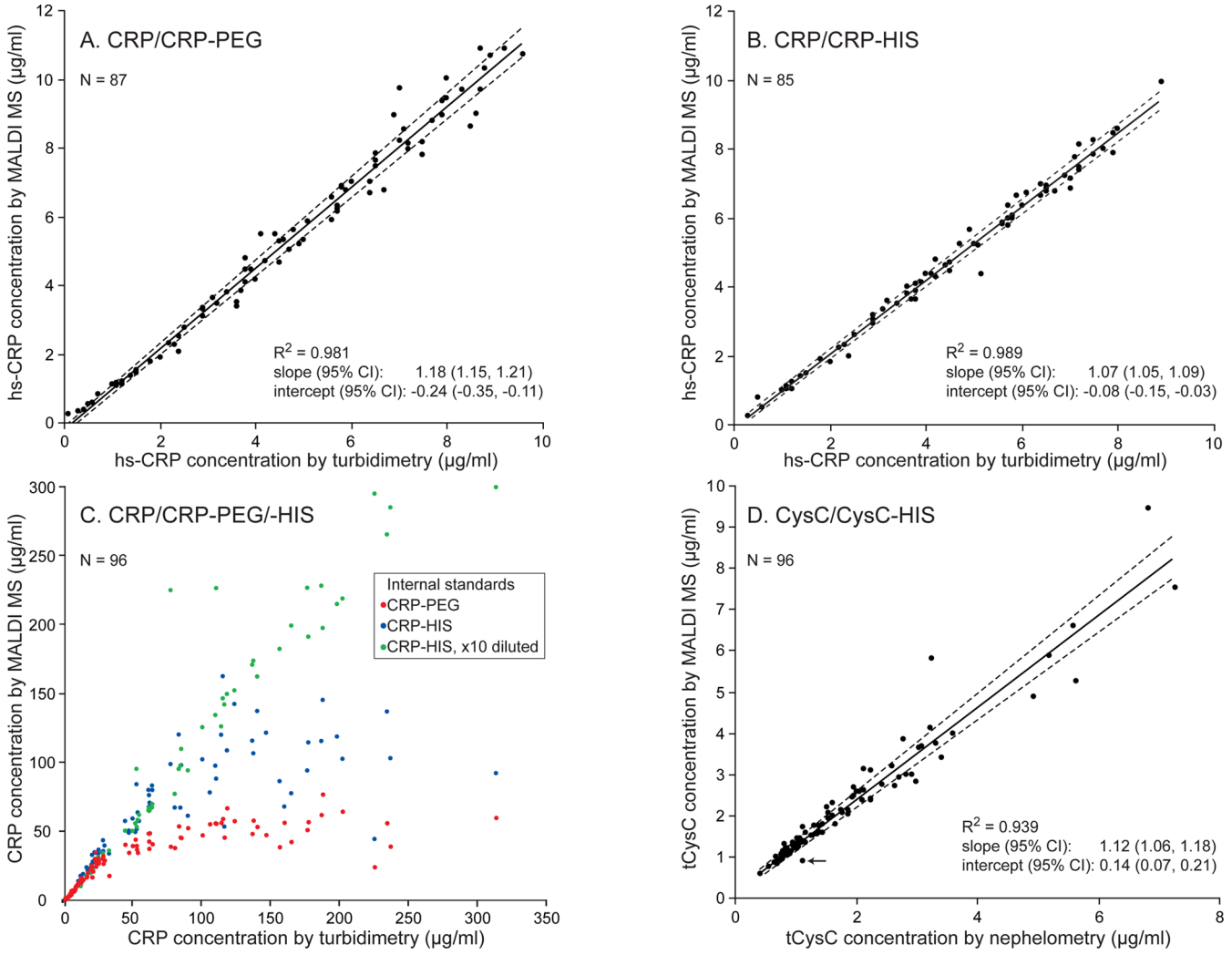

Figure 3. Comparison between immuno-MALDI-MS and reference methods using Passing–Bablok regression. Between-assay agreement was evaluated by two different sets of reference samples. The first set of 87 clinical serum samples, with known hs-CRP concentration obtained by turbidimetry, was analyzed by immuno-MALDI-MS with CRP-PEG (A) or CRP-HIS (B) as the internal standard. Comparisons demonstrate linear relationships between both methods with significant differences in the slope and intercepts from one and zero, respectively. The polyhistidine-tagged IS again performed better than the PEGylated IS. A second set of reference samples ($N = 96$) covering the larger concentration range was quantified for CRP and cystatin C. Immuno-MALDI-MS was performed as a singleplex assay for CRP using CRP-PEG as the IS and as a duplex assay of CRP and cystatin C using the polyhistidine-tagged standards. Quantification of CRP using CRP-PEG (C) shows the linear relationship with turbidimetry for concentrations below 30 μg/mL. At higher levels the curve reaches a plateau probably due to column saturation in immuno-MALDI-MS. Saturation is also observed for quantification using the CRP-HIS standard, although it starts at higher levels of about 70 μg/mL. Sample dilution with PBS by a factor of 10 prevents column saturation and enables a linear relationship over the entire CRP range. The last panel (D) shows the Passing–Bablok regression for total cystatin C and demonstrates the linear relationship between immuno-MALDI-MS and nephelometry with significant differences in the slope and intercepts from one and zero, respectively.

cant deviations in slope and intercepts for both methods. Deviations in terms of 95% confidence intervals (CIs) (slope; intercept) were smaller using polyhistidine-labeled (1.05, 1.09; −0.15, −0.03) than PEG-labeled (1.15, 1.21; −0.35, −0.11) internal standards. The Bland–Altman plots (Supporting Information Figure S-2A) confirm the higher performance of the polyhistidine-labeled IS compared to the PEGylated IS in terms of bias (CRP/CRP-HIS vs CRP/CRP-PEG, 2.5% vs 10.7%) and 95% CI [(+23%, −18%) vs (+34%, −13%)]. In addition, the plots show that the bias increased with higher levels of CRP.

A second set of reference samples was analyzed by immuno-MALDI-MS and included wide concentration ranges of CRP (0.1–311.9 μg/mL) and cystatin C (0.4–7.3 μg/mL). The relationship between values obtained with the CRP/CRP-PEG assay and turbidimetry was linear for [CRP] < 30 μg/mL, but leveled off at higher concentration to reach a plateau at about 60 μg/mL (Figure 3C, red symbols). A similar relationship was observed for the CRP/CRP-HIS assay (Figure 3C, blue symbols), except that the plateau appeared at levels >70 μg/mL. This suggests saturation of CRP affinity sites and a somewhat higher binding capacity for polyhistidine-tagged than PEG-tagged IS. The binding capacity of a ZipTip is typically 5 μg of protein, which is about 3×10^{-11} mol of antibody.[63] However, this may be the maximum value, since the amount of inactive antibody by denaturation or sterical blockage is unknown. To extend the analytical range, serum samples were diluted in PBS by a factor of 10, and a linear relationship (R^2 = 0.938, CI_{slope} = (1.13, 1.21), CI_{inter} = (−1.76, −0.26)) was

dx.doi.org/10.1021/ac500704y | Anal. Chem. 2014, 86, 5807–5814

achieved over the entire concentration range (Figure 3C, green symbols).

Levels of cystatin C determined by immuno-MALDI-MS and nephelometry were compared in Figure 3D. The total cystatin C (tCysC) was determined for immuno-MALDI-MS by summing up the peak intensities of all cystatin C isoforms and was compared to that determined from nephelometry, which does not distinguish between the native and modified forms of cystatin C. Notably, this summation is only correct if all CysC isoforms possess the same antigenicity to anti-CysC and comparable detection probabilities in MALDI-MS. Passing–Bablok regression showed good between-assay agreement (R^2 = 0.939), although the 95% CI for the slope (1.06, 1.18) and intercept (0.07, 0.21) differed significantly from 1 and 0, respectively. The relatively high CI of the slope may be explained by diverse antibody specificities of both methods to cystatin C isoforms. The Bland–Altman plot (Supporting Information Figure S-2B) demonstrates a 19.8% higher average tCysC by immuno-MALDI-MS compared to nephelometry. The 95% CI ranged from +43% to −4%. The bias between immuno-MALDI-MS and nephelometry decreased with higher levels of tCysC.

Quantification of Cystatin C Variants. The concentrations of cystatin C isoforms were determined for the reference data set and are plotted against the sample number (Supporting Information Figure S-3), sorted by increasing levels of total cystatin C (black line, right axis). The graph demonstrates the interindividual variation of the different isoforms with average concentrations (percentage) of 0.85 μg/mL (39.0%) for CysC-3ProOH, 0.74 μg/mL (33.9%) for the native form, 0.26 μg/mL (11.9%) for des-S CysC-3ProOH, 0.21 μg/mL (9.6%) for des-S CysC, and 0.11 μg/mL (5.0%) for des-SSP CysC. Data from Trenchevska et al.[19] showed similar amounts for native cystatin C (36.0%) and des-S CysC (9.2%), but higher amounts for CysC-3ProOH (46.2%) and des-SSP CysC (8.7%). However, comparison could be improper, since Trenchevska et al. did not quantify the des-S CysC-3ProOH variant and analyzed samples of lower average tCysC levels. In addition, we observed that the ratio of CysC to CysC-3ProOH was inversely related to the tCysC levels (ρ = −0.344, p = 0.001). Among the 96 reference samples we analyzed, one sample showed an unknown variant causing a mass shift of −57.8 Da for all cystatin C isoforms (data not shown), which may be caused by a novel point mutation.

CONCLUSION

In this study, we have described a novel duplex immuno-MALDI approach for the sensitive and accurate quantification of CRP and cystatin C. Several isoforms were detected for cystatin C, which could be quantified. There are other immunoaffinity-based MS techniques for the targeted quantification of proteins, such as iMALDI[17] and SISCAPA MRM LC-MS/MS,[18] but these techniques quantify proteins on the basis of peptide fragments and thus are not able or require multiple analyses to determine protein modifications. In contrast, the combination of immunoaffinity enrichment and intact protein detection allows quantitative evaluation of microheterogeneity for several target proteins in a single analysis. Most methods use covalently linked antibodies, which make them labor-intensive. Our method involves simple antibody immobilization based on reversed-phase material and represents an alternative approach if interferences of the target proteins with background signals, i.e., albumin and antibody fragments, can be avoided. In addition, we could demonstrate that modified recombinant target proteins can serve as internal standards for competitive immuno-MALDI assays. The high throughput and the low sample consumption make this method well suited for assessment of biomarker status based on samples from large and precious biobanks. Further assay optimization will enhance assay efficiency by higher levels of multiplexing.

ASSOCIATED CONTENT

Supporting Information

Additional information as described in text. This material is available free of charge via the Internet at http://pubs.acs.org.

AUTHOR INFORMATION

Corresponding Author

*E-mail: klaus.meyer@bevital.no.

Notes

The authors declare no competing financial interest.

ACKNOWLEDGMENTS

We thank Terje Ertkjær from The Laboratorium for Klinisk Biokjemi of the Haukeland University Hospital and Katrin Borucki from The Institut fur Klinische Chemie of the Otto von Guericke University Magdeburg for collection and analyses of the reference serum samples.

REFERENCES

(1) Rai, A. J. *Expert Rev. Mol. Diagn.* **2007**, *7*, 545–553.
(2) Alvarez-Llamas, G.; de la Cuesta, F.; Barderas, M. E.; Darde, V.; Padial, L. R.; Vivanco, F. *Expert Rev. Proteomics* **2008**, *5*, 679–691.
(3) Jenab, M.; Slimani, N.; Bictash, M.; Ferrari, P.; Bingham, S. A. *Hum. Genet.* **2009**, *125*, 507–525.
(4) Singh, V.; Martinezclark, P.; Pascual, M.; Shaw, E. S.; O'Neill, W. W. *Coron. Artery Dis* **2010**, *21*, 244–256.
(5) Sim, S. C.; Ingelman-Sundberg, M. *Trends Pharmacol. Sci.* **2011**, *32*, 72–81.
(6) Prabakaran, S.; Lippens, G.; Steen, H.; Gunawardena, J. *Wiley Interdiscip. Rev.: Syst. Biol. Med.* **2012**, *4*, 565–583.
(7) Arnaudo, A. M.; Garcia, B. A. *Epigenet. Chromatin* **2013**, *6*, 24.
(8) Lothrop, A. P.; Torres, M. P.; Fuchs, S. M. *FEBS Lett.* **2013**, *587*, 1247–1257.
(9) Patel, D. J.; Wang, Z. *Annu. Rev. Biochem.* **2013**, *82*, 81–118.
(10) Nedelkov, D.; Kiernan, U. A.; Niederkofler, E. E.; Tubbs, K. A.; Nelson, R. W. *Proc. Natl. Acad. Sci. U.S.A.* **2005**, *102*, 10852–10857.
(11) Kiernan, U. A. *Expert Rev. Proteomics* **2007**, *4*, 421–428.
(12) Leng, S. X.; McElhaney, J. E.; Walston, J. D.; Xie, D.; Fedarko, N. S.; Kuchel, G. A. *J. Gerontol. A: Biol. Sci. Med. Sci.* **2008**, *63*, 879–884.
(13) Marquette, C. A.; Corgier, B. P.; Blum, L. J. *Bioanalysis* **2012**, *4*, 927–936.
(14) Roepstorff, P. *Protein Cell* **2012**, *3*, 641–647.
(15) Bantscheff, M.; Lemeer, S.; Savitski, M. M.; Kuster, B. *Anal. Bioanal. Chem.* **2012**, *404*, 939–965.
(16) Nikolov, M.; Schmidt, C.; Urlaub, H. *Methods Mol. Biol.* **2012**, *893*, 85–100.
(17) Jiang, J.; Parker, C. E.; Fuller, J. R.; Kawula, T. H.; Borchers, C. H. *Anal. Chim. Acta* **2007**, *605*, 70–79.
(18) Anderson, L.; Hunter, C. L. *Mol. Cell Proteomics* **2006**, *5*, 573–588.
(19) Trenchevska, O.; Nedelkov, D. *Proteome Sci.* **2011**, *9*, 19.
(20) Maiolica, A.; Junger, M. A.; Ezkurdia, I.; Aebersold, R. *J. Proteomics* **2012**, *75*, 3495–3513.
(21) Boja, E. S.; Rodriguez, H. *Proteomics* **2012**, *12*, 1093–1110.
(22) Weiss, F.; van den Berg, B. H.; Planatscher, H.; Pynn, C. J.; Joos, T. O.; Poetz, O. *Biochim. Biophys. Acta, Proteins Proteomics* **2014**, *1844*, 927–932.
(23) Patrie, S. M.; Mrksich, M. *Anal. Chem.* **2007**, *79*, 5878–5887.

(24) Chou, P. H.; Chen, S. H.; Liao, H. K.; Lin, P. C.; Her, G. R.; Lai, A. C.; Chen, J. H.; Lin, C. C.; Chen, Y. J. *Anal. Chem.* **2005**, *77*, 5990−5997.
(25) Wang, K. Y.; Chuang, S. A.; Lin, P. C.; Huang, L. S.; Chen, S. H.; Ouarda, S.; Pan, W. H.; Lee, P. Y.; Lin, C. C.; Chen, Y. J. *Anal. Chem.* **2008**, *80*, 6159−6167.
(26) Nelson, R. W.; Krone, J. R.; Bieber, A. L.; Williams, P. *Anal. Chem.* **1995**, *67*, 1153−1158.
(27) Nelson, R. W.; Borges, C. R. *J. Am. Soc. Mass Spectrom.* **2011**, *22*, 960−968.
(28) Palmblad, M.; Bindschedler, L. V.; Cramer, R. *Proteomics* **2007**, *7*, 3462−3469.
(29) Kilpatrick, E. L.; Liao, W. L.; Camara, J. E.; Turko, I. V.; Bunk, D. M. *Protein Expression Purif.* **2012**, *85*, 94−99.
(30) Tubbs, K. A.; Kiernan, U. A.; Niederkofler, E. E.; Nedelkov, D.; Bieber, A. L.; Nelson, R. W. *Anal. Chem.* **2006**, *78*, 3271−3276.
(31) Eisenhardt, S. U.; Thiele, J. R.; Bannasch, H.; Stark, G. B.; Peter, K. *Cell Cycle* **2009**, *8*, 3885−3892.
(32) Windgassen, E. B.; Funtowicz, L.; Lunsford, T. N.; Harris, L. A.; Mulvagh, S. L. *Postgrad. Med.* **2011**, *123*, 114−119.
(33) Hirschfield, G. M.; Pepys, M. B. *QJM* **2003**, *96*, 793−807.
(34) Casas, J. P.; Shah, T.; Hingorani, A. D.; Danesh, J.; Pepys, M. B. *J. Intern. Med.* **2008**, *264*, 295−314.
(35) Hingorani, A. D.; Shah, T.; Casas, J. P.; Humphries, S. E.; Talmud, P. J. *Clin. Chem.* **2009**, *55*, 239−255.
(36) Kaptoge, S.; Di Angelantonio, E.; Lowe, G.; Pepys, M. B.; Thompson, S. G.; Collins, R.; Danesh, J. *Lancet* **2010**, *375*, 132−140.
(37) Di Napoli, M.; Elkind, M. S.; Godoy, D. A.; Singh, P.; Papa, F.; Popa-Wagner, A. *Expert Rev. Cardiovasc. Ther.* **2011**, *9*, 1565−1584.
(38) Allin, K. H.; Bojesen, S. E.; Nordestgaard, B. G. *J. Clin. Oncol.* **2009**, *27*, 2217−2224.
(39) Allin, K. H.; Nordestgaard, B. G. *Crit. Rev. Clin. Lab. Sci.* **2011**, *48*, 155−170.
(40) Saito, K.; Kihara, K. *Nat. Rev. Urol.* **2011**, *8*, 659−666.
(41) Devaraj, S.; Singh, U.; Jialal, I. *Curr. Opin. Lipidol.* **2009**, *20*, 182−189.
(42) Pravenec, M.; Kajiya, T.; Zidek, V.; Landa, V.; Mlejnek, P.; Simakova, M.; Silhavy, J.; Malinska, H.; Oliyarnyk, O.; Kazdova, L.; Fan, J.; Wang, J.; Kurtz, T. W. *Hypertension* **2011**, *57*, 731−737.
(43) Angelidis, C.; Deftereos, S.; Giannopoulos, G.; Anatoliotakis, N.; Bouras, G.; Hatzis, G.; Panagopoulou, V.; Pyrgakis, V.; Cleman, M. W. *Curr. Top. Med. Chem.* **2013**, *13*, 164−179.
(44) Zhang, Z.; Lu, B.; Sheng, X.; Jin, N. *Am. J. Kidney Dis.* **2011**, *58*, 356−365.
(45) Odutayo, A.; Cherney, D. *Clin. Nephrol.* **2012**, *78*, 64−75.
(46) Taglieri, N.; Koenig, W.; Kaski, J. C. *Clin. Chem.* **2009**, *55*, 1932−1943.
(47) Sekizuka, H.; Akashi, Y. J.; Kawasaki, K.; Yamauchi, M.; Musha, H. *J. Cardiol.* **2009**, *54*, 359−367.
(48) Hojs Fabjan, T.; Penko, M.; Hojs, R. *Renal Failure* **2014**, *36*, 81−86.
(49) Vigil, L.; Lopez, M.; Condes, E.; Varela, M.; Lorence, D.; Garcia-Carretero, R.; Ruiz, J. *J. Am. Soc. Hypertens.* **2009**, *3*, 201−209.
(50) Levy, E.; Jaskolski, M.; Grubb, A. *Brain Pathol.* **2006**, *16*, 60−70.
(51) Wilson, M. E.; Boumaza, I.; Lacomis, D.; Bowser, R. *PLoS One* **2010**, *5*, e15133.
(52) Fiorini, M.; Zanusso, G.; Benedetti, M. D.; Righetti, P. G.; Monaco, S. *Proteomics Clin Appl.* **2007**, *1*, 963−971.
(53) Cathcart, H. M.; Huang, R.; Lanham, I. S.; Corder, E. H.; Poduslo, S. E. *Neurology* **2005**, *64*, 755−757.
(54) Nedelkov, D.; Shaik, S.; Trenchevska, O.; Aleksovski, V.; Mitrevski, A.; Stojanoski, K. *Open Proteomics J.* **2008**, *1*, 54−58.
(55) Galteau, M. M.; Guyon, M.; Gueguen, R.; Siest, G. *Clin. Chem. Lab. Med.* **2001**, *39*, 850−857.
(56) Woloshin, S.; Schwartz, L. M. *N. Engl. J. Med.* **2005**, *352*, 1611−1613.
(57) Applied Biosystems. *Application Note TOF MS*; Foster City, CA, 2002.
(58) Wenzel, T.; Sparbier, K.; Mieruch, T.; Kostrzewa, M. *Rapid Commun. Mass Spectrom.* **2006**, *20*, 785−789.
(59) Armbruster, D. A.; Pry, T. *Clin. Biochem. Rev.* **2008**, *29* (Suppl.1), S49−52.
(60) Passing, H.; Bablok, W. *J. Clin. Chem. Clin. Biochem.* **1983**, *21*, 709−720.
(61) Bland, J. M.; Altman, D. G. *Lancet* **1986**, *1*, 307−310.
(62) Kiernan, U. A.; Nedelkov, D.; Niederkofler, E. E.; Tubbs, K. A.; Nelson, R. W. *Methods Mol. Biol.* **2006**, *328*, 141−150.
(63) Millipore. *User Guide for Reversed-Phase ZipTip*; Billerica, MA, 2007.